

Cell Reports, Volume 24

Supplemental Information

Flow Cytometry of Mouse and Human

Adipocytes for the Analysis of Browning

and Cellular Heterogeneity

Carolina E. Hagberg, Qian Li, Maria Kutschke, Debajit Bhowmick, Endre Kiss, Irina G. Shabalina, Matthew J. Harms, Olga Shilkova, Viviana Kozina, Jan Nedergaard, Jeremie Boucher, Anders Thorell, and Kirsty L. Spalding

Figure S1.

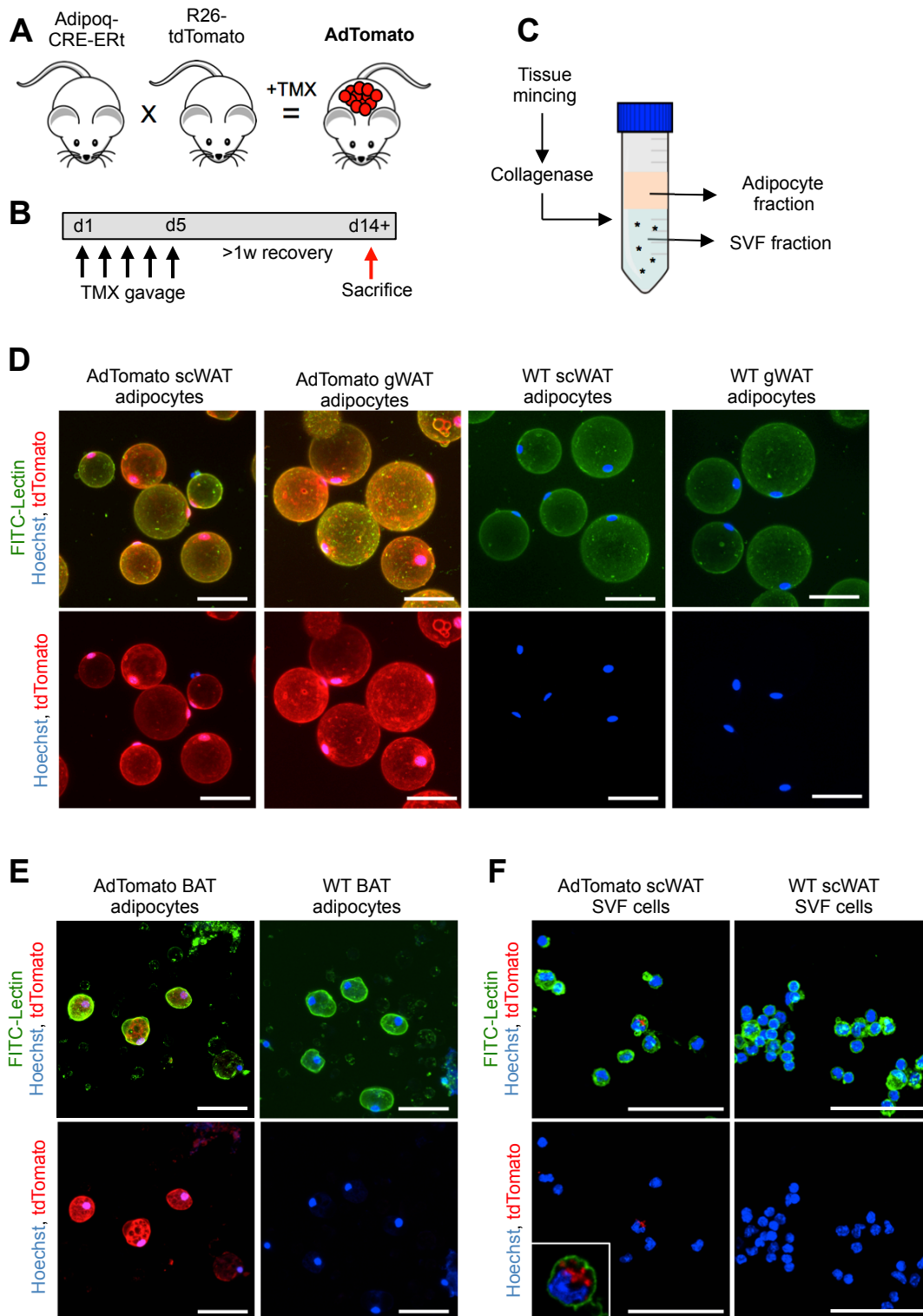


Figure S1. Characterization of AdTomato adipocytes. Related to Figure 1.

(A) Schematic diagram showing the generation of AdTomato mice through breeding and oral gavage with tamoxifen (TMX).

(B) Timeline for TMX gavage and sacrifice of AdTomato mice.

(C) Schematic diagram depicting the isolation process for adipocytes and SVF cells.

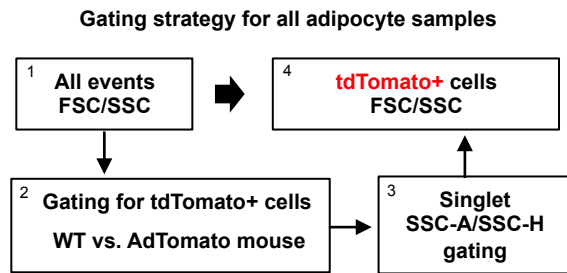
(D) Enlarged images of FITC-lectin- (green) and Hoechst- (blue) stained scWAT and gWAT adipocytes isolated from AdTomato and WT mice.

(E) FITC-lectin- (green) and Hoechst- (blue) stained isolated BAT adipocytes from AdTomato and WT mice.

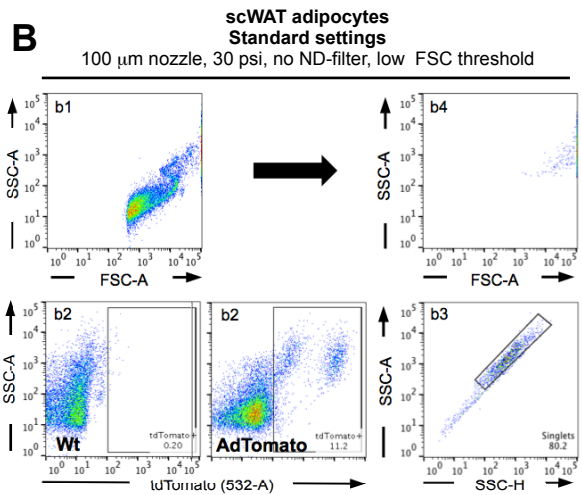
(F) Zoomed images of FITC-lectin- (green) and Hoechst- (blue) stained SVF cells isolated from scWAT from AdTomato and WT mice. All scale bars are 50 μm , note the differences in length.

Figure S2.

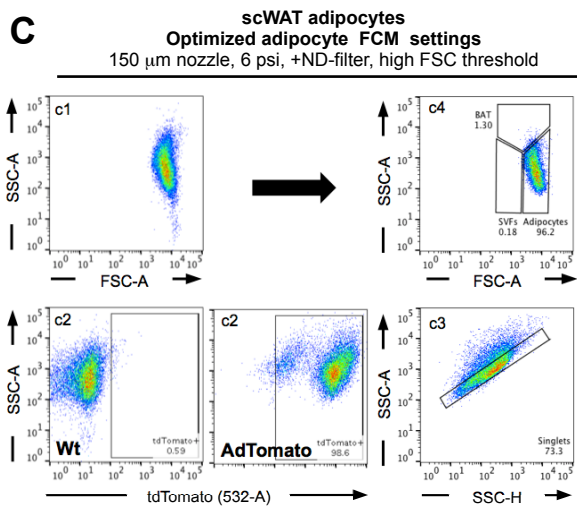
A



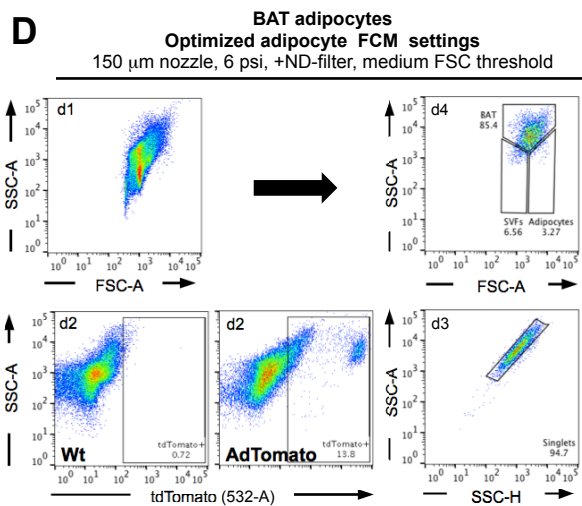
B



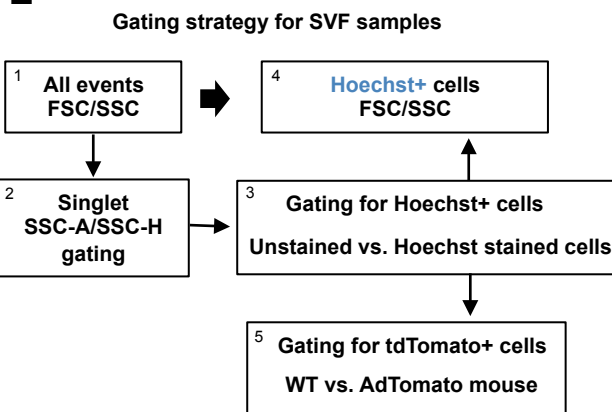
C



D



E



F

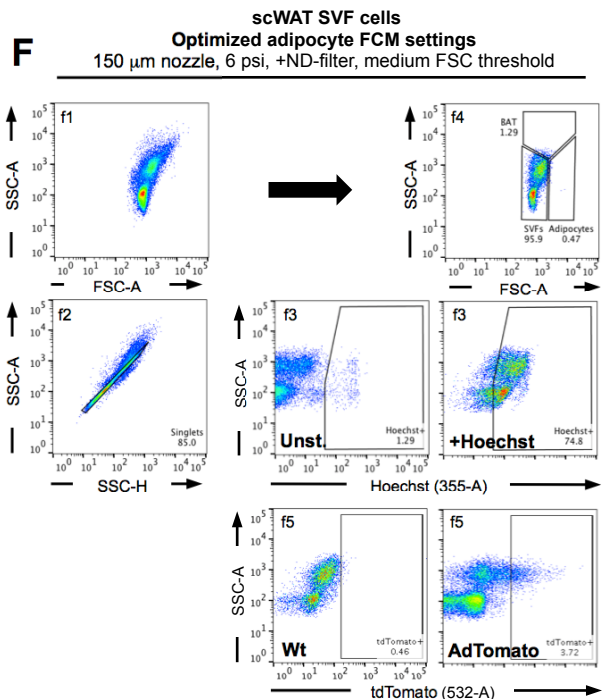


Figure S2. Detailed gating strategy for adipocytes and SVF cells. Related to Figure 1.

(A) Schematic depicting the step-by-step flow cytometry gating strategy for AdTomato adipocyte samples used throughout the study. TdTomato and singlet gated adipocyte samples are shown on FSC/SSC in the last step.

(B-D) Representative graphs showing flow cytometry gating for a scWAT sample run using standard settings (B), the same scWAT sample run using optimized settings (C) and for BAT samples run using optimized settings (D). Note the existence of two separate tdTomato+ populations (b2/c2/d2), which also are visible by confocal imaging (Figure S1D).

(E) Schematic diagram depicting the step-by-step flow cytometry gating strategy for SVF samples used throughout the study. Singlet and Hoechst gated SVF samples are shown on FSC/SSC in the last step.

(F) Representative graphs showing flow cytometry gating for a SVF sample run using optimized settings.

Table S1. Related to Figure 1 and 2.

Critical settings	Why?	If not...	Possible solutions and alternatives*
ND-filter in FSC channel	Allows visualization of large cells on FSC	FSC saturation and no detection of mature adipocytes on FSC/SSC	Some machines offer the possibility to add ND-filters manually. Lowering laser power does not help.
High threshold on FSC	Hides small events like debris and lipid droplets, improving adipocyte detection	Analysis is possible but the adipocyte % will be low due to masking by the large number of lipids in samples	Available in all machines
In tube stirring	Allows sampling of adipocytes by stirring the cells into solution	No white adipocytes enter the flow cytometry machine	Beckman Coulter Smart Sampler or home made solution with external stirring
Additional settings to consider	Why?	If not...	Possible solutions and alternatives*
Large nozzle and lower pressure	Prevents adipocyte breakage and facilitates sorting of intact cells	Non-optimal analysis and sorting conditions, possible adipocyte breakage	Use analyser with large cuvette size
Ambient temperature	Low temperature affects lipid fluidity, stiffening the stored lipids within the adipocytes	Increased cell breakage, lowering yield	Available in most machines
Staining with DNA dye	Allows detection of adipocytes and discards lipid droplets, specially in BAT	Makes it harder to gate for BAT adipocytes	Use e.g. Hoechst, DyeCycle dyes or Draq5

*For the latest flow cytometry solutions on the market we recommend to contact your local company salesperson

Table S1. Critical settings for flow cytometric analysis of mature adipocytes as well as additional flow cytometry settings worth considering.

Figure S3.

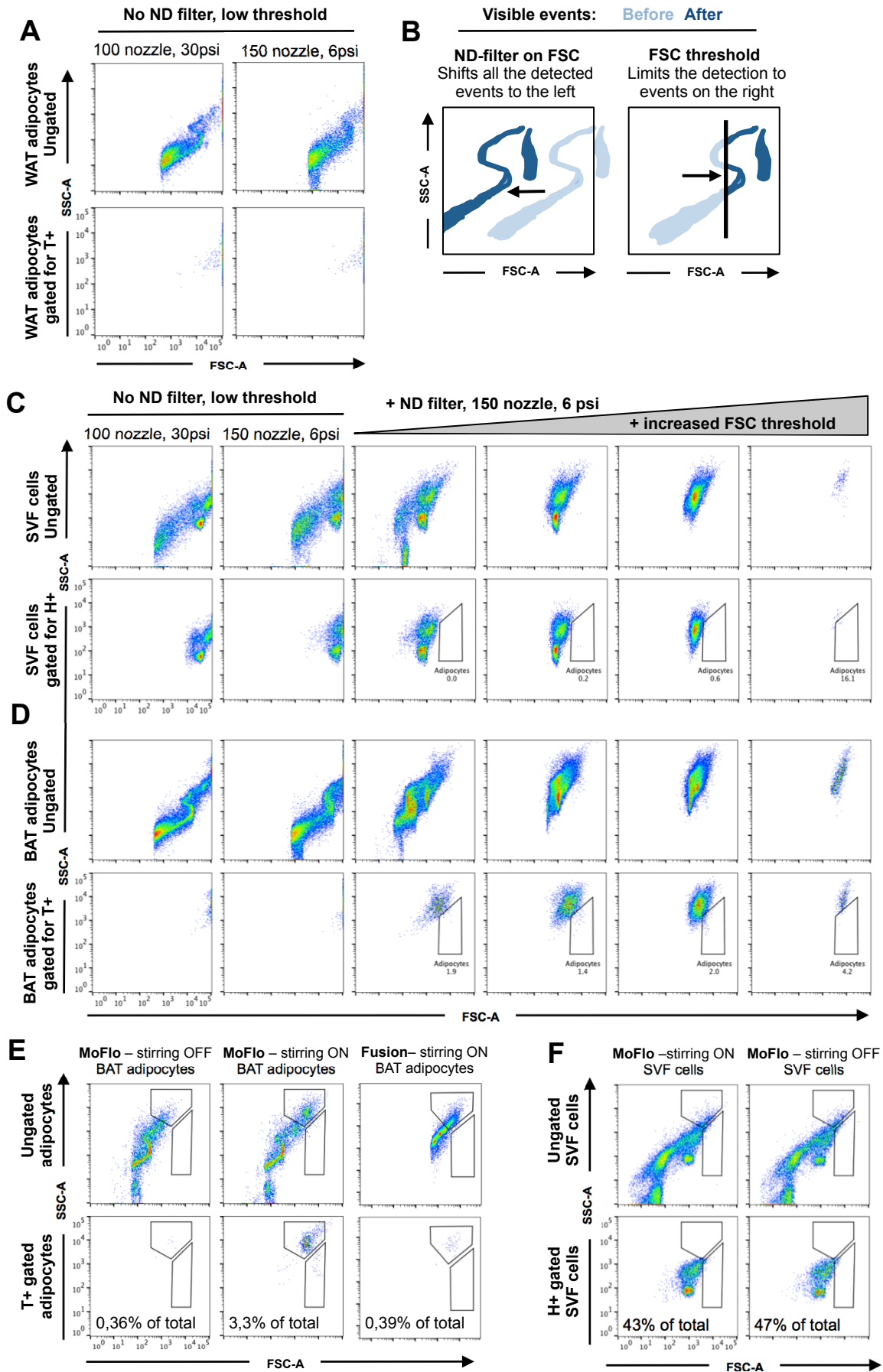


Figure S3. Effect of nozzle, ND-filter and threshold on adipocyte and SVF samples analyzed by flow cytometry. Related to Figure 2.

(A) Adipocyte samples analyzed with either a 100 μm nozzle and 30 psi or a 150 μm nozzle and 6 psi in the absence of a ND filter on FSC, showing ungated or tdTomato+ (T+) gated events.

(B) Schematic drawing of the effect of a FSC ND filter and increased FSC thresholding. Note that increasing the FSC threshold only hides smaller events but does not change the position of a specific population.

(C) SVF samples showing ungated or Hoechst+ (H+) gated events when run with different nozzles without a ND-filter on FSC (first and second column), after inserting an ND-filter using the 150 μm nozzle (2nd column) and with ND-filter plus increasing FSC thresholds (3rd and 4th columns).

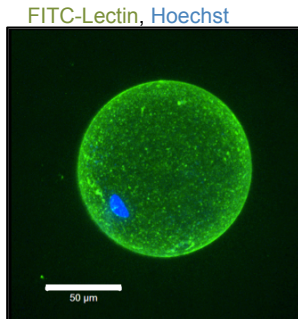
(D) BAT samples showing ungated or Tomato+ (T+) gated events when run using the same settings as in (C).

(E) Ungated mouse BAT adipocytes run using the Beckman MoFlo XDP cell sorter with the in-tube stirring turned OFF or ON, or run using the BD Fusion cell sorter that has a rotational stirring mechanism. All samples were acquired using a low threshold to visualize the lipid droplets. Note that few cells within the *Adipocyte* population are detected when stirring is turned off or when only rotational stirring is available.

(F) Ungated mouse SVF cell sample run using the Beckman MoFlo XDP cell sorter with the in-tube stirring turned OFF or ON.

Figure S4.

A Sorted from human scWAT



B Sorted unfixed mouse cells

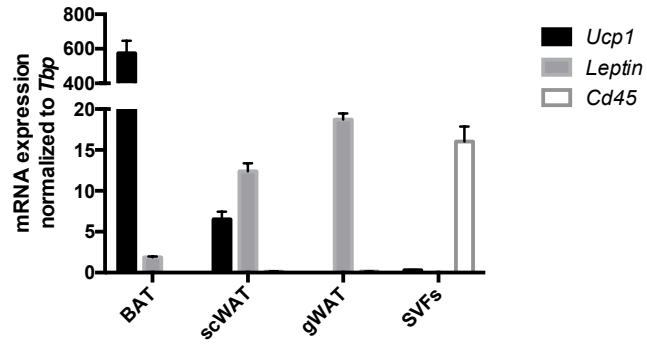


Figure S4. Sorting human and mouse adipocytes. Related to Figure 3.

- (A) Confocal stack showing representative image of a sorted, intact human scWAT adipocyte.
- (B) Relative mRNA expression of *Ucp1*, *Leptin* and *Cd45* in sorted cell fractions from BAT, scWAT, gWAT and SVF samples, compared to *Tbp* expression.

Figure S5.

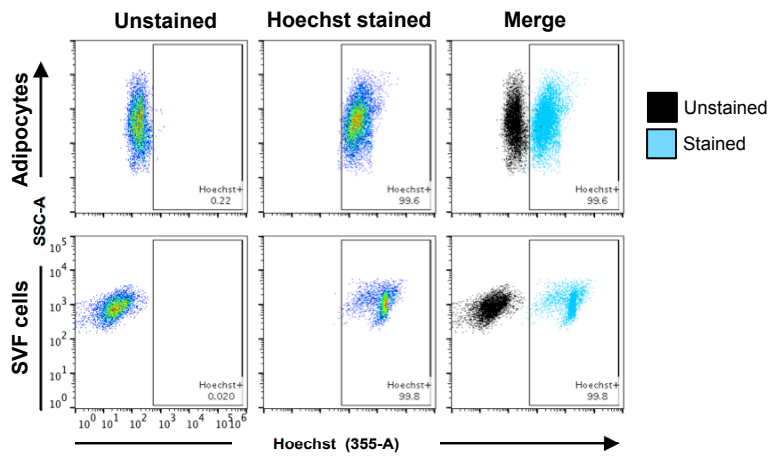


Figure S5. Staining adipocyte and SVF samples with Hoechst. Related to Figure 5. Representative graphs showing unstained and Hoechst-stained adipocytes (top) and SVF cells (bottom) stained with an equal Hoechst concentration for the same amount of time, plots are also shown merged. Note the difference in how much the events shift between cell types. Adipocytes were gated using the Adipocyte and singlet gating, SVFs were singlet gated.

Figure S6.

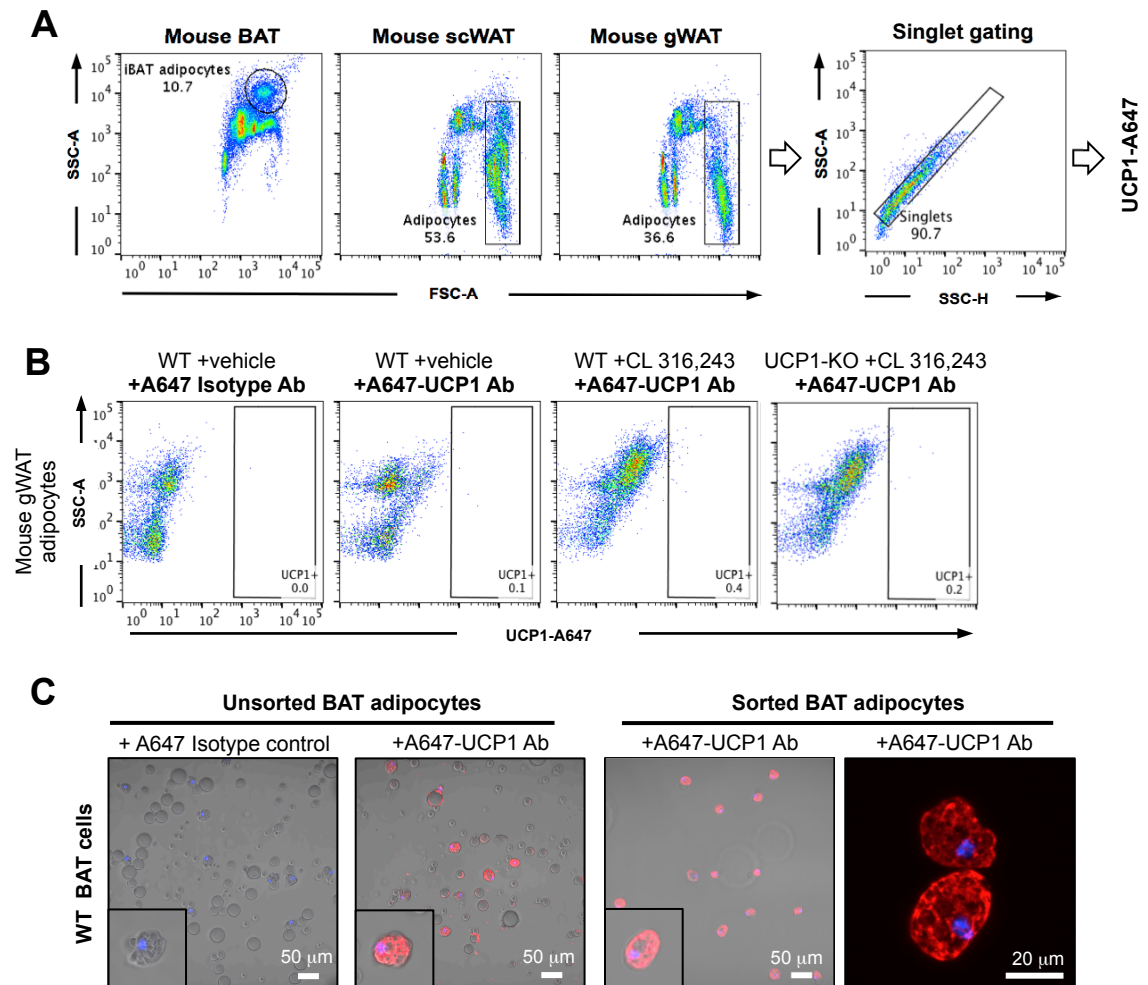


Figure S6. Antibody validation and gating strategy for UCP1 immunocytochemistry. Related to Figure 6.

(A) Representative graphs depicting the gating strategy used to analyze UCP1 staining. Adipocytes from WAT were first detected on FSC/SSC using the *Adipocyte* gate, subsequently singlet gated using SSC-A and SSC-H, and analyzed for UCP1 staining as shown in Figure 6. Adipocytes from BAT were identified on FSC/SSC based on previous gating experiments (see Figure S2D).

(B) Flow cytometric analysis of gWAT adipocytes from untreated or CL 316,243-treated WT or UCP1-KO mice stained with isotype control or anti-UCP1 antibody.

(C) Representative images showing unsorted BAT cells from WT mice stained with isotype control or with UCP1 antibody. The same BAT adipocyte sample is shown after sorting of UCP1-expressing cells. Note the disappearance of the large amount of sample debris following sorting.

Figure S7.

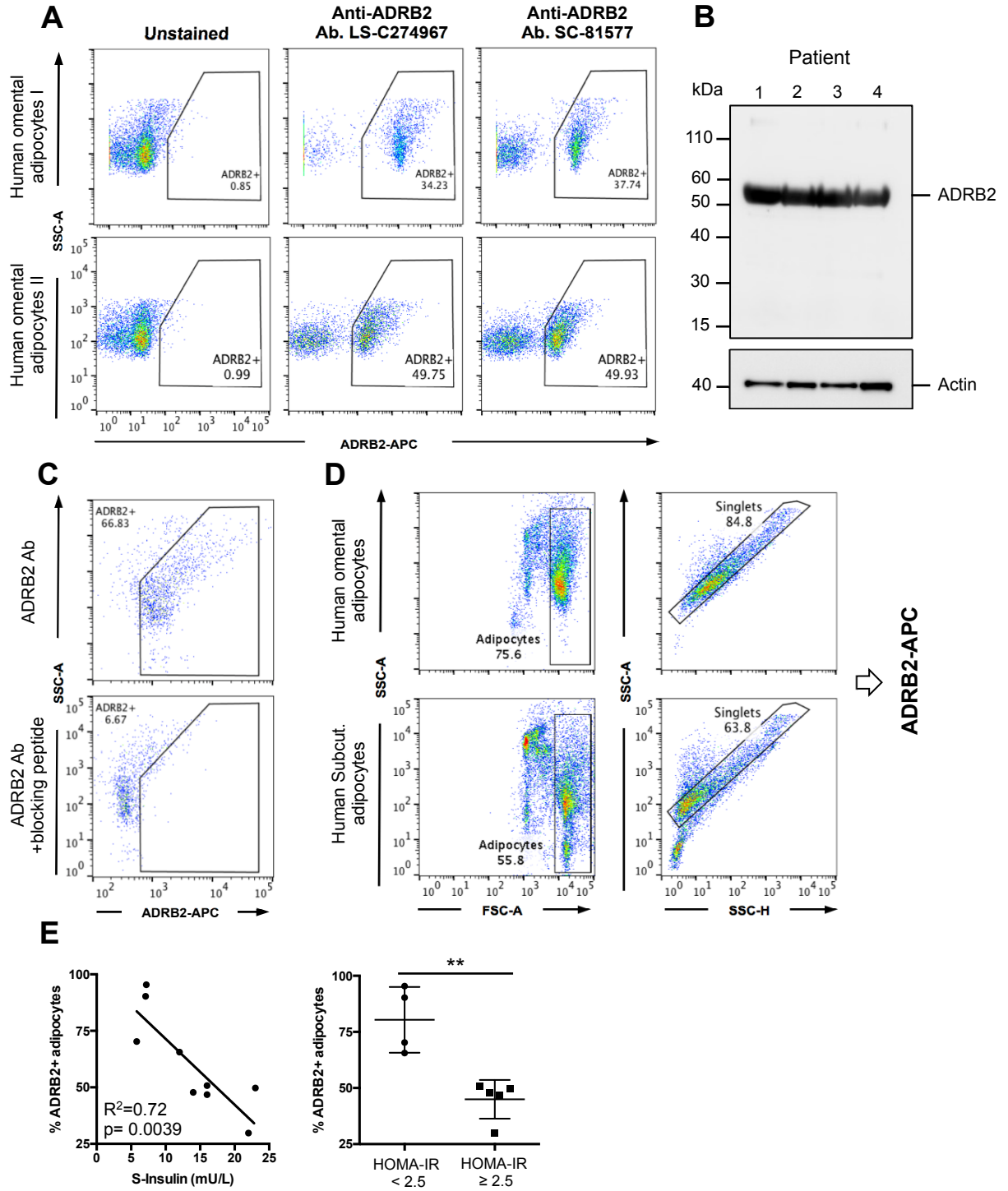


Figure S7. Validation of ADRB2 antibody and gating strategy for analyzing human adipocytes by flow cytometry. Related to Figure 7.

(A) Flow cytometric analysis of two human omWAT adipocyte samples unstained or stained with two different conjugated anti-ADRB2 antibodies.

(B) Western blot of omWAT adipocytes from four patients (#1-4) organized in order of increasing HOMA-IR index and detected for ADRB2. Actin was detected as a loading control.

(C) Flow cytometric analysis of omWAT adipocytes stained with antibody only, or with antibody that has been pre-incubated with a 5x molar excess of specific blocking peptide (lower panel).

(D) Representative graphs depicting the gating strategy used to analyze human adipocytes by flow cytometry. Human scWAT and omWAT adipocytes were first detected on FSC/SSC using the *Adipocyte* gate, subsequently singlet gated using SSC-A and SSC-H, and analyzed for beta-adrenergic receptor 2 (ADRB2) expression as shown in Figure 7.

(E) Correlation of the percentage of omWAT ADRB2+ cells with patient fasting S-insulin levels (left) as well as comparison of the percentage of omental adipocytes expressing ADRB2 between metabolically healthy (HOMA-IR index < 2.5) and metabolically unhealthy obese patients. Bar shows mean ± standard deviation.